Available online at www.sciencedirect.com
ScienceDirect
Journal of the European Ceramic Society 31 (2011) 1581–1588
www.elsevier.com/locate/jeurceramsoc

A new in situ process in precision casting for mold fabrication

Eun-Hee Kim [a,*], Jae-Hyun Lee [a], Yeon-Gil Jung [a,**], Chang-Seop Lee [b], Ungyu Paik [c]

[a] School of Nano and Advanced Materials Engineering, Changwon National University, #9 Sarim-dong, Changwon, Kyungnam 641-773, Republic of Korea
[b] Technical Research Department, METIA Corporation, #192-7 Shinchon-dong, Changwon, Kyungnam 641-773, Republic of Korea
[c] Department of Energy Engineering, Hanyang University, Haengdang-dong, Sungdong-Gu, Seoul 133-791, Republic of Korea

Received 3 December 2010; received in revised form 28 February 2011; accepted 7 March 2011
Available online 16 April 2011

Abstract

A new in situ process for mold fabrication in precision casting has been developed to decrease processing time and production costs, and produce an environmentally friendly mold, compared with the conventional process. In the new process, the starting powder is fastened by an inorganic binder, whereas the mold in the conventional process takes its form by using an organic binder. The fixing of powders by the inorganic binder is caused by a sol–gel reaction of precursor materials. Therefore, the new mold process is more environmentally friendly and simpler than the conventional process. The inorganic binder system for the in situ process was prepared from a mixture of tetraethyl orthosilicate and poly(dimethyl siloxane) as SiO_2 precursor, and sodium methoxide as Na_2O precursor. The prepared samples show a fracture strength of about 5 MPa, indicating that the in situ process can be applied to the fabrication of molds having high mechanical properties.

Keywords: Composites; Firing; Microstructure-final; Mold; Precursors-organic; Sol–gel processes

1. Introduction

Recently, the convert mold process in precision casting, which uses a mixture of alkyl silicate and sodium alkoxide, has been introduced to fabricate shell molds.[1,2] This convert mold process has many advantages, such as high strength, enhancement of collapse, easy processability, and high thermal stability, making it useful in many different applications, for example, in automobiles, and aerospace materials. Typically, mold fabrication has been accomplished using the convert mold process of six steps: (1) a coating process of starting materials with an organic binder, (2) preparation of the mold by heat treatment at 200 °C, (3) a dipping process into inorganic binder precursors, (4) a first drying process at 80 °C, (5) a second drying process at 200 °C, and (6) heat treatment at 1000 °C, resulting in the conversion of the organic-bonded mold to the inorganic-bonded mold.[3-5] The new method for mold fabrication has several advantages, such as a decrease in the processing time and production costs and the production of an environmentally friendly mold, due to the omission of three of the above steps, (1), (3), and (5) in the convert mold process using.

The new mold process introduced in this work is called an in situ process because the mold can be prepared by direct mixing starting powder and inorganic binder. The binder system for fabricating the mold by the in situ process was prepared with tetraethyl orthosilicate (TEOS) and poly(dimethyl siloxane) (PDMS) as a precursor of silicon dioxide (SiO_2) and sodium methoxide (NaOMe) as a precursor of sodium oxide (Na_2O). The mold could be shaped by a solid-state phase reaction (SiO_2, Na_2CO_3) generated by the sol–gel reaction of TEOS and NaOMe during a drying process. These sol–gel reactions were investigated as functions of binder composition and viscosity of the SiO_2 precursor in an attempt to study the mechanical properties of the prepared mold and the reactivity of the precursor, considering the differences between the mold-fixing effects of the organic and inorganic binders. The relationship between strength and binder composition is discussed based on the microstructures observed.

2. Experimental details

A composite binder for the new in situ process was prepared using two types of SiO_2 precursor: tetraethyl orthosilicate (η(viscosity) = 0.0179 cP at 25 °C, Sigma–Aldrich Korea,

* Corresponding author. Tel.: +82 55 213 2742; fax: +82 55 262 6486.
** Corresponding author. Tel.: +82 55 213 3712; fax: +82 55 262 6486.
E-mail addresses: udam99@changwon.ac.kr (E.-H. Kim), jungyg@changwon.ac.kr (Y.-G. Jung).

0955-2219/$ – see front matter © 2011 Elsevier Ltd. All rights reserved.
doi:10.1016/j.jeurceramsoc.2011.03.013

Table 1
The chemical composition and various physical properties of starting powder.

Chemical composition (%)		Porosity (%)	Bulk specific gravity	Water absorption (%)
Al_2O_3	60.59	2.2	2.72	0.8
SiO_2	36.44			
Fe_2O_3	1.08			
TiO_2	0.72			
CaO	0.20			
MgO	0.08			
K_2O	0.20			
Na_2O	0.35			
P_2O_5	0.27			
Total	99.93			

Table 2
Formulations of binder systems to prepare the mold in processes I and II.

Process	Run number	TEOS [wt%]	PDMS [wt%]	PVA [wt%]	NaOMe [wt%]	Isobutyl alcohol [wt%]
I	1	38	–		56	6
	2[a], 3[b]	30.4	7.6		56	6
II	4[a], 5[b]	30.4	7.6	1	56	6
	6[b]	–	38	1	56	6

[a] Viscosity (η) of PDMS used is 25 cSt.
[b] Viscosity (η) of PDMS used is 200 cSt.

Yongin, Korea) of silicate type with hydrolysis and condensation reactions (sol–gel reaction), and poly(dimethyl siloxane) (PDMS, $\eta = 25$ and 200 cSt at 25 °C, $\rho = 0.95$–0.97 g/ml, Sigma–Aldrich Korea, Yongin, Korea) of siloxane type without the sol–gel reaction. The SiO_2 precursor mixtures were prepared by mixing the silicate and/or siloxane types. Sodium methoxide (NaOMe, Sigma–Aldrich Korea, Yongin, Korea) and 10% poly(vinyl alcohol) aqueous solution (PVA, $\eta = 450$ cP at 25 °C, Sigma–Aldrich Korea, Yongin, Korea) were used as the precursors of Na_2O and organic binder, respectively. Powder with complex composition (Cerabeads, nominal particle size 0.39 mm, Seto, Japan), which is an artificial ceramic sand, was used as a starting powder. The chemical composition and fundamental physical properties of starting powder are shown in Table 1. In this work, two different methods were employed for preparing the mold samples: in one method, the starting powder was simply fixed by glassification of the inorganic binder (process I), in particular TEOS with the sol–gel reaction; in the other method, the organic binder was added in an appropriate composition to prepare the sample (process II), in particular PDMS without the sol–gel reaction. The powders mixed with precursors with and without organic binder were formed using a high pressure of 60 MPa with a cuboid shape of $10 \times 10 \times 50\ mm^3$. The formed samples were dried at 80 °C for 1 h, and then heat-treated at 1000 °C for 1 h. In addition, in the case of process II, the starting powders was heat-treated at 80 °C for 0.5 h before forming, owing to the evaporation of water used to dissolve the PVA. Schematic diagrams for the new in situ methods without (process I) and with (process II) the organic binder are shown in Fig. 1. The basic formulations and experimental ranges of binder systems to prepare the shell mold through the in situ process are shown in Table 2. The hydrolysis reaction of the precursor mate-

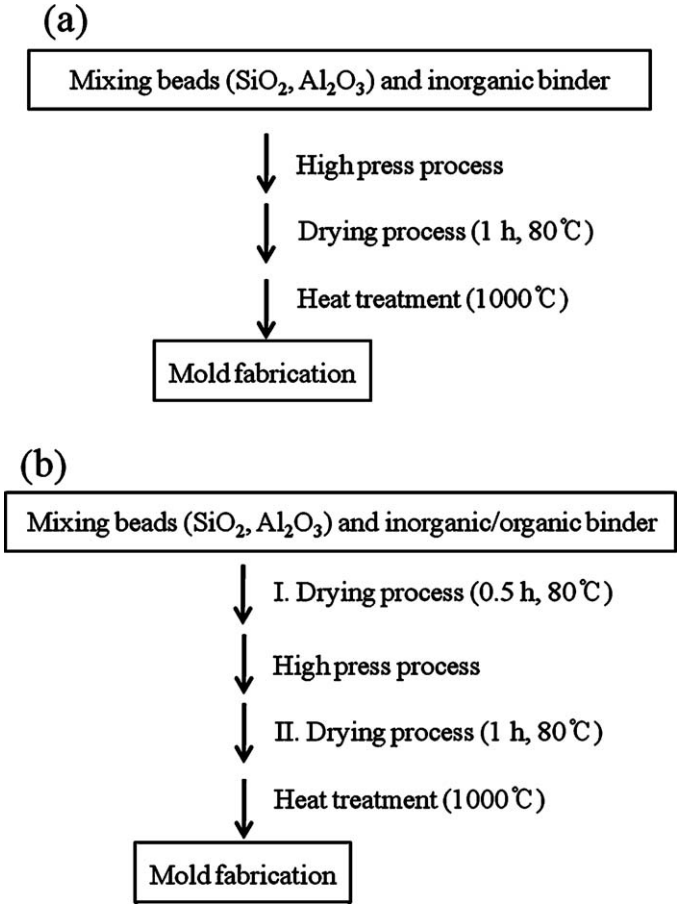

Fig. 1. Schematic diagram of mold fabrication for precision casting: (a) process I and (b) process II.

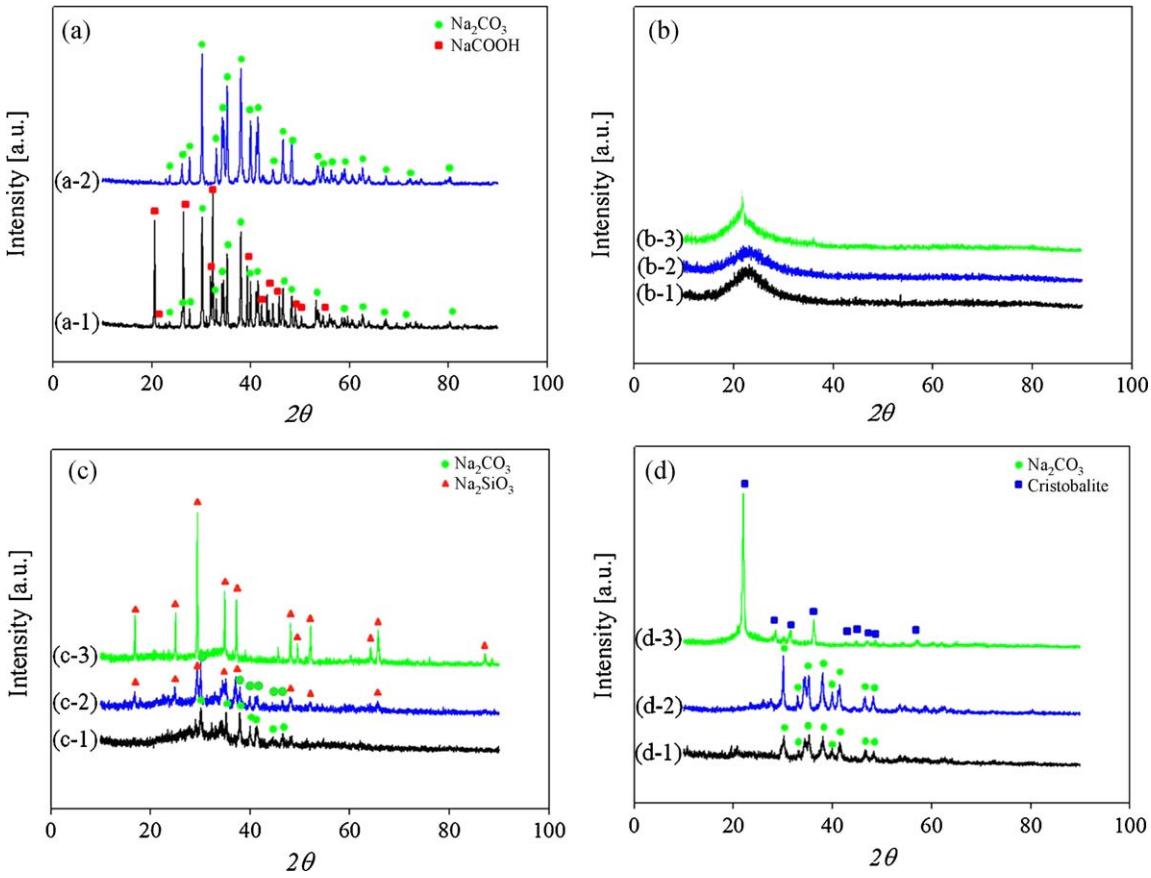

Fig. 2. XRD patterns of precursors after the hydrolysis reaction and heat treatment: (a) NaOMe, (b) TEOS, (c) mixture of TEOS and NaOMe, and (d) mixture of PDMS (25 cSt) and NaOMe. Each number indicates XRD patterns after hydrolysis, heat treatment at 500 °C, and heat treatment at 1000 °C, respectively. (For interpretation of the references to color in this figure legend, the reader is referred to the web version of the article.)

rials used in this work was carried out by the addition of water at 80 °C for 1 h, and then the hydrolyzed precursors were heat-treated under two temperature conditions, 500 and 1000 °C, for 1 h to define the glassification behavior by reaction of sodium hydroxide (NaOH) and SiO_2 during heat treatment.

The change of precursors after hydrolysis and the heat treatment was analyzed using a Fourier transform infrared spectrometer (FT-IR, Nicolet, Thermo Fisher Scientific, Waltham, MA, USA) and an X-ray diffractometer (XRD, Philips X-pret MPD, Model PW3040, Eindhoven, Netherlands). The fracture morphology and microstructure were observed using a scanning electron microscope (JEOL Model JSM-5610, Tokyo, Japan), and the elemental analysis of each sample was carried out using an energy dispersive X-ray spectrometer (energy resolution = 133 eV, Oxford Inst., Oxford, UK). The fracture strength of the samples after heat treatment was measured using a universal testing machine (Instron 5566, Instron Corp., Norwood, MA, USA) in a four-point bending mode at a rate of 0.5 mm min^{-1}. Tests were carried out at room temperature, and at least five runs were performed to determine the standard deviation of the strength.

3. Results and discussion

Fig. 2 presents XRD profiles of the precursor materials with the sol–gel reaction (NaOMe and TEOS) and mixture precursor materials (TEOS + NaOMe and PDMS + NaOMe), showing materials after the hydrolysis reaction and after heat treatment under two conditions, 500 °C and 1000 °C. In Fig. 2(a), first NaOMe is converted into NaOH by the hydrolysis reaction, and then NaOH is again transformed into Na_2CO_3 (sodium carbonate) and NaOOCH (sodium formate). However, the NaOOCH peak completely disappeared after heat treatment at 500 °C, and no material remained after treatment at 1000 °C caused by the complete decomposition of Na_2CO_3. The XRD patterns of TEOS used as the SiO_2 precursor are shown in Fig. 2(b). TEOS is changed into amorphous SiO_2 during the hydrolysis reaction, which is very stable and independent of the heat treatment temperature. Consequently, TEOS and NaOMe could be used for forming the mold because of the relatively fast and stable glassification.[6–8] In the mixture of TEOS and NaOMe, the XRD result shows complex peaks of Na_2CO_3 generated from NaOMe and amorphous SiO_2 from TEOS after hydrolysis (Fig. 2(c)). Then, these products are changed into the glass phase of Na_2SiO_3 (sodium silicate) at 1000 °C *via* a complex mixture of Na_2CO_3, amorphous SiO_2, and Na_2SiO_3 under heat treatment at 500 °C. However, results of the mixture containing PDMS and NaOMe (Fig. 2(d)) are significantly different from the results of the mixture with TEOS and NaOMe because of the PDMS without the hydrolysis reaction. After the hydrolysis reaction, the mixture with PDMS and NaOMe shows only the peak from Na_2CO_3. Moreover, as the mixture with PDMS and

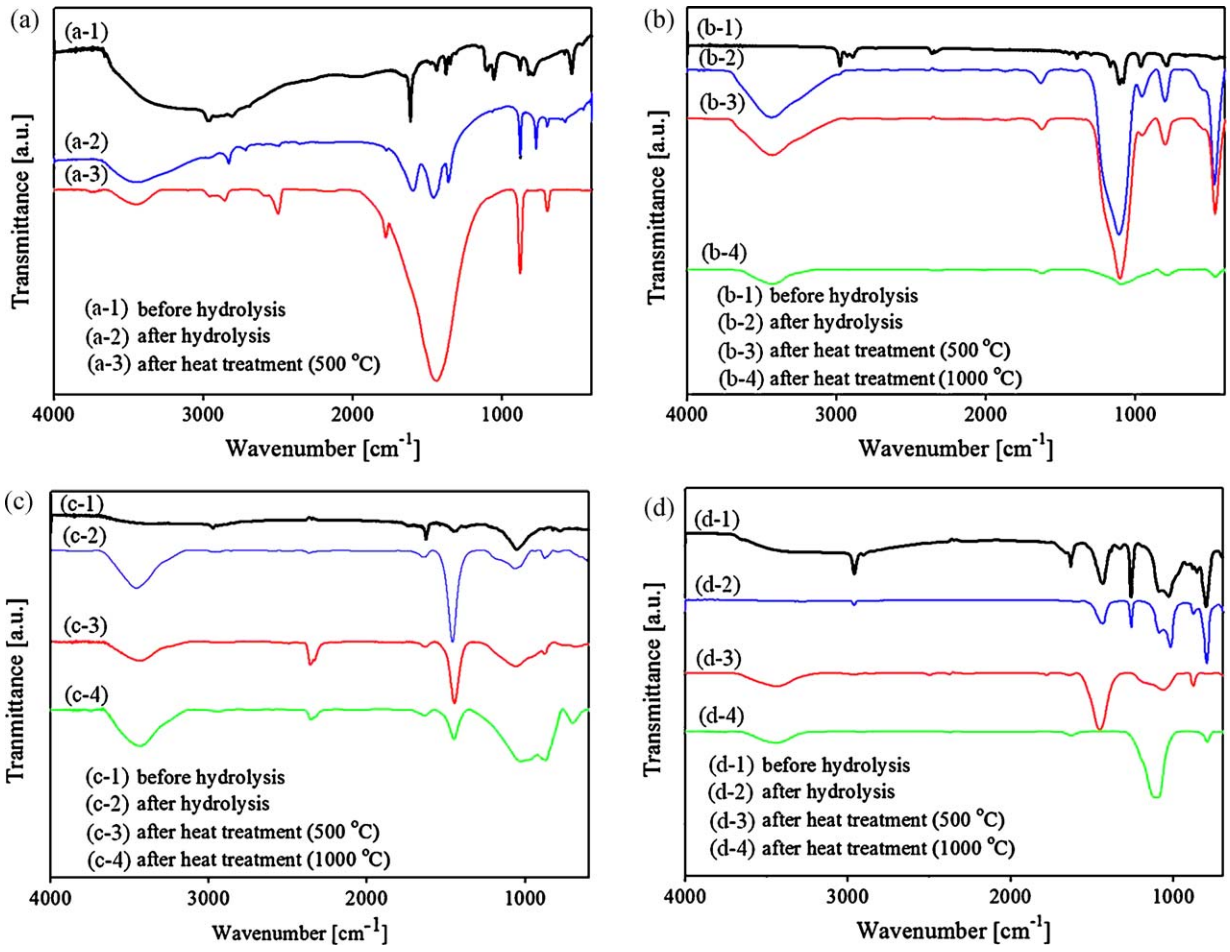

Fig. 3. FT-IR spectra of precursors used in this work: (a) NaOMe, (b) TEOS, (c) mixture of TEOS and NaOMe, and (d) mixture of PDMS (25 cSt) and NaOMe. Each number indicates FT-IR spectra before hydrolysis, after hydrolysis, before heat treatment at 500°C, and after heat treatment at 1000°C.

NaOMe is heat-treated at 1000 °C, PDMS is converted into the crystal phase of cristobalite along with complete degradation of Na_2CO_3. However, in the case of heat treatment at 500 °C, the XRD pattern shows complex peaks of Na_2CO_3 and amorphous SiO_2.

FT-IR spectra of various precursor materials, such as TEOS, PDMS, and mixture materials (TEOS + NaOMe and PDMS + NaOMe) are shown in Fig. 3, with varies conditions: (1) before hydrolysis reaction, (2) after hydrolysis reaction, (3) after heat treatment at 500 °C, and (4) after heat treatment at 1000 °C. Fig. 3(a) shows the products of NaOMe treated under various conditions. Na_2CO_3 after the hydrolysis reaction and the heat treatment has the specific characteristic peaks of CO_3^{2-} at 1400 and 900 cm^{-1}. In addition, any FT-IR peaks related to NaOMe do not appear after treatment at 1000 °C, as indicated in Fig. 3(a). In Fig. 3(b), the TEOS peak before the hydrolysis reaction shows two characteristic bands at 2800–3000 cm^{-1} and 1000 cm^{-1}, which are assigned to the C–H stretching vibration by the ethyl group and Si–O stretching peak, respectively. However, after the hydrolysis reaction and the heat treatment, the C–H stretching peak disappears and a peak arising from the Si–OH group occurring at 3500 cm^{-1} is observed. In addition, the Si–O–Si group bending peak occurring at 470 cm^{-1} is observed.[9] These results confirm that TEOS undergoes two reactions: (1) the formation of Si–OH by the hydrolysis reaction with water, and (2) a condensation reaction between Si–OH groups after the hydrolysis reaction, which is principally the sol–gel process.[10,11] In addition, the generated amorphous SiO_2 does not vary under any reaction conditions (hydrolysis reaction, heat treatment at 500 and 1000 °C), as seen in Fig. 2(b). In Fig. 3(c), FT-IR spectra of the mixture with TEOS and NaOMe simply show a mixture of neat NaOMe and TEOS before the hydrolysis reaction. However, after the hydrolysis reaction and the heat treatment, it is seen that peaks arise from the CO_3^{2-}, Si–OH group, and Si–O stretching peak occurring at 1400, 3500, and 1000 cm^{-1}, respectively, indicating peaks of SiO_2 and Na_2CO_3. The characteristic bands arising from PDMS show an Si–OH stretching peak occurring at 3500 cm^{-1}, a C–H stretching peak occurring at 2800–3000 cm^{-1}, sharp and strong Si–O–Si stretching peaks occurring at 800 and 1100 cm^{-1}, and an Si–CH_3 stretching vibration occurring at 1250 cm^{-1} (Fig. 3(d)).[12,13] The PDMS peaks do not change after the hydrolysis reaction. The variations before and after the hydrolysis reaction are due solely to NaOMe. This suggests that PDMS does not undergo the sol–gel reaction, resulting in a high efficiency binder system. PDMS has a molecular structure that contains Si–O–Si linkages, whereas TEOS forms these linkages after undergoing the sol–gel reaction, as shown in Fig. 3. Therefore, a significant difference in the

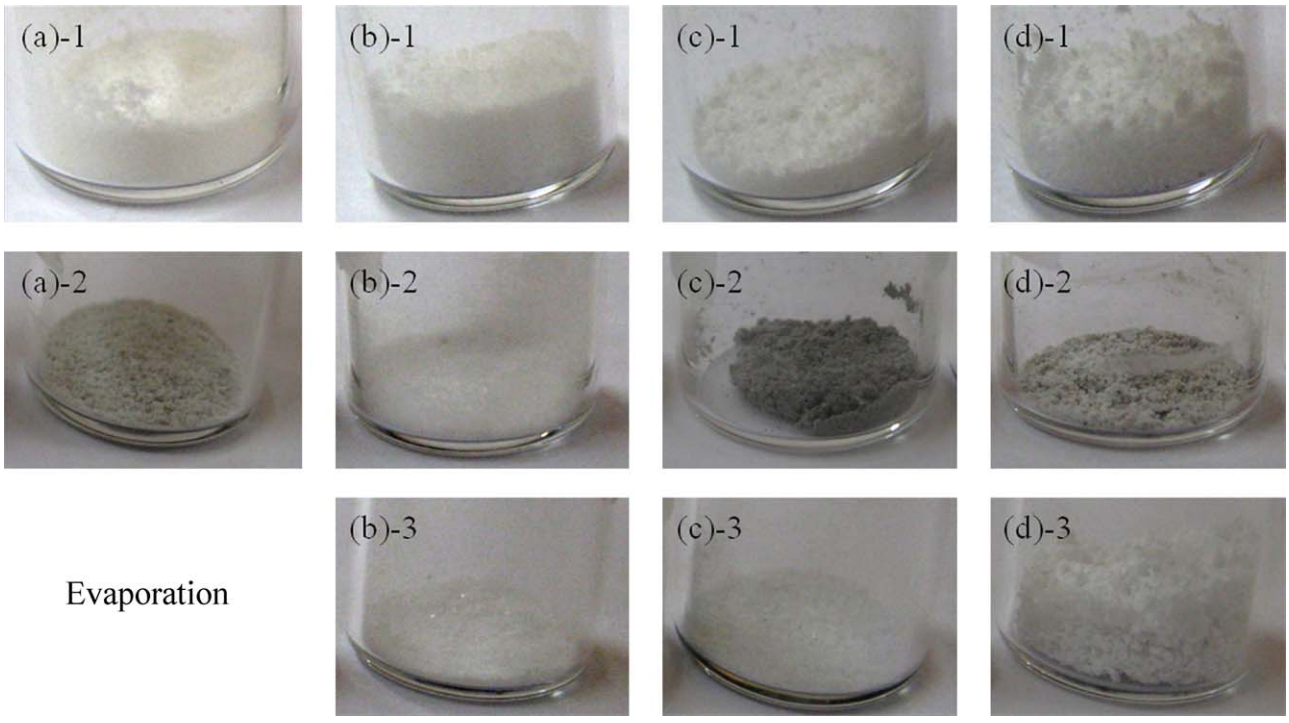

Fig. 4. Photographs of precursors after the hydrolysis reaction and the heat treatment: (a) NaOMe, (b) TEOS, (c) mixture of TEOS and NaOMe, and (d) mixture of PDMS (25 cSt) and NaOMe. Each number indicates the precursor materials after the hydrolysis reaction (series 1), after the heat treatment at 500 °C (series 2), and after the heat treatment at 1000 °C (series 3).

spectra before and after the hydrolysis reaction is observed in Fig. 3(c), while a similar spectrum is shown in Fig. 3(d) except for the peak occurring at 1600 cm^{-1} resulting from the NaOMe.

Photographs of the precursor materials after the hydrolysis reaction and the heat treatment are shown in Fig. 4. NaOMe, TEOS, and the mixture of TEOS and NaOMe are converted from a transparent liquid into white solid products after the hydrolysis reaction. However, the mixture of PDMS and NaOMe becomes a gel phase by mixing the neat PDMS of liquid phase with the white solid Na_2CO_3 after the hydrolysis reaction. The product heat-treated at 500 °C shows gray powders owing to Na_2CO_3 without chemical bonding with SiO_2, except for TEOS. During the heat treatment at 1000 °C, neat Na_2CO_3 is completely burned and the others show a white glass phase, contributing to the fracture strength of the mold.

The fracture morphology and microstructure of each sample with different binder compositions are shown in Fig. 5; these are obtained at the fracture surface after the bending strength tests. Generally, precursors are converted into a white solid during the drying and heat treatment processes, as proved in Fig. 4. Namely, this white area (reaction area) is the SiO_2 phase from PDMS and the Na_2SiO_3 phase made by reaction between TEOS and NaOMe, as shown in Fig. 2. All samples formed by process I show an apparent reaction area resulting from the Na_2SiO_3 and/or the SiO_2 (Fig. 5(a)–(c)), whereas in the case of those by process II, the white solid is not localized but uniformly spread over the entire sample (Fig. 5(d)–(f)). The content of the precursor in the sample is decreased by generation of sodium silicate (Na_2SiO_3) during the drying and heat-treatment processes. In particular, the content of the precursor is sharply decreased at the surface of the sample having a high reactivity. This reduction causes a decrease in the chemical potential related to diffusion of the precursor, in accordance with the following equation:[14]

$$\mu_i = \mu_i^0 + RT \ln x_i \quad (1)$$

where μ_i, μ_i^0, R, T, and x_i are the chemical potential of component i in solution and a pure phase, gas constant, temperature, and mole fraction of component i, respectively. The chemical potential of each precursor is similar in the equilibrium state. During the process, unreacted precursor is moved to the reaction area (surface of the sample) to reduce the difference in chemical potential between the reaction area and the non-reaction area. Therefore, a chemical potential gradient is formed from the surface to the inside of sample. The reaction area of samples made by process I does not vary significantly with precursor structure, indicating that the strengths of the samples are similar. However, in the case of process II, the Na_2SiO_3 and SiO_2 phases are generated in the whole sample because of the difficult migration of precursor within matrix, resulting from the high viscosity of the organic binder (PVA). The diffusion coefficient (D) is inversely proportional to the viscosity of the mixture as:[15,16]

$$D = \frac{k_B T}{6\pi\eta_o R} \quad (2)$$

where k_B T, η_o, and R are the Boltzmann constant, temperature, η_o viscosity, and molecular radius, respectively. With increasing viscosity of the mixture, diffusion of molecules becomes more difficult. Therefore, in the case of addition of PVA, reaction of the precursor would take place over the whole sample.

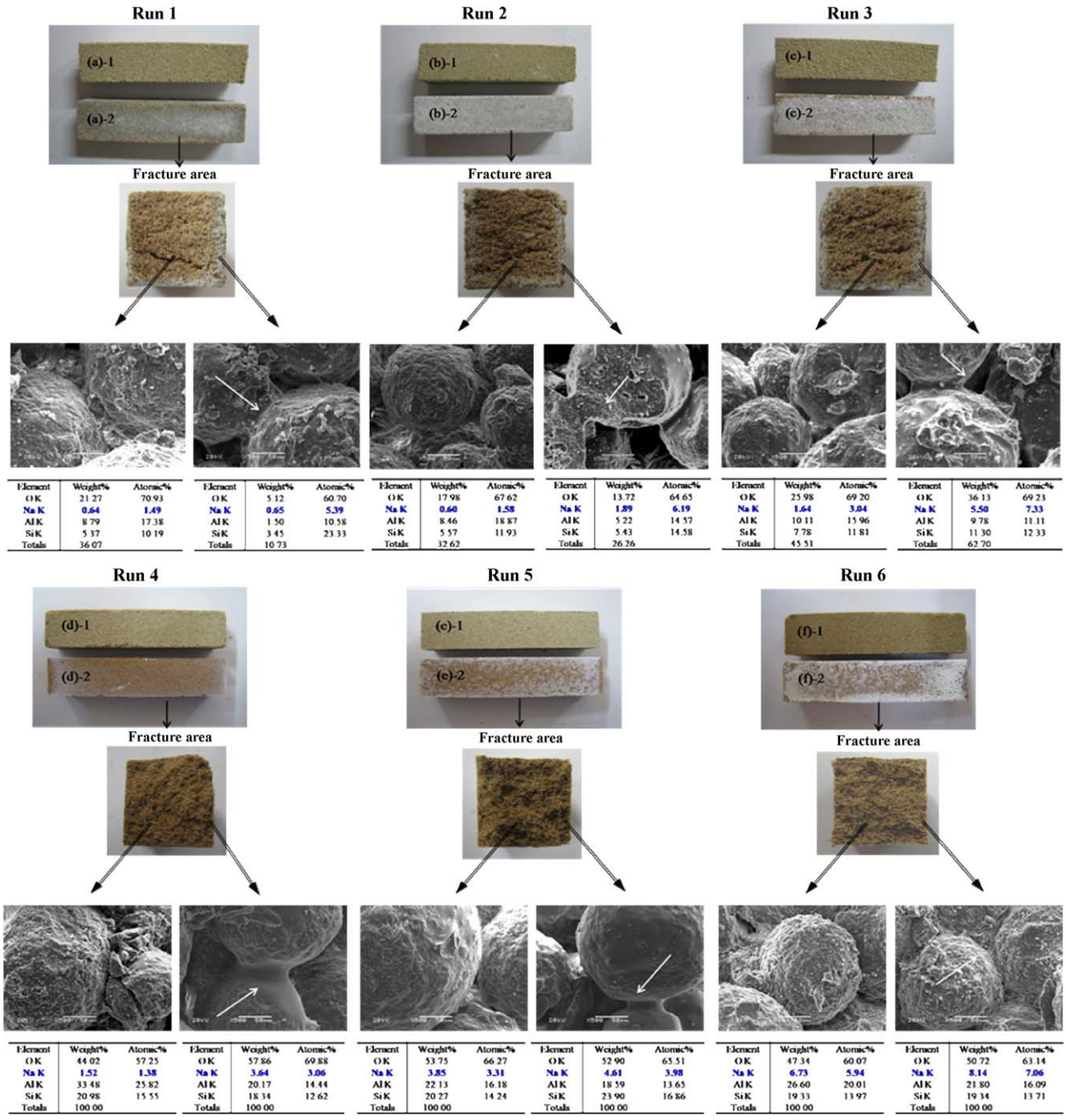

Fig. 5. Fracture morphologies and microstructure of each sample before (series 1) and after (series 2) heat treatment as a function of binder composition.

In this work, the glass phase converted by the inorganic binder is observed at the interface and surface of powders, indicated by white arrows in Fig. 5. The surface of sample is more glassified than the inner region because the concentration of Na is higher at the surface than the inside of sample. The binder composition has no influence on the fracture morphology and microstructure, meaning that it is not directly related to fracture strength.

The results of element analysis of the sample based on the binder composition mixed with PDMS ($\eta = 200$ cSt) and TEOS and NaOMe (Run 3), before and after the heat treatment, are shown in Fig. 6. After the heat treatment, the concentrations of Na and Si are decreased from the surface to the inside of sample, whereas those before the heat treatment have similar values throughout the sample. This is because the precursor can migrate as a result of the high reactivity of the surface during the heat treatment.

The fracture strength of samples fabricated from different binder compositions was measured after the heat treatment; the results are shown in Fig. 7. In the case of samples formed by process I, the strength values are similar, independent of the binder composition. However, samples prepared by process II show different strength values as a function of binder composition. Generally, the viscosity of mixture has an influence on the

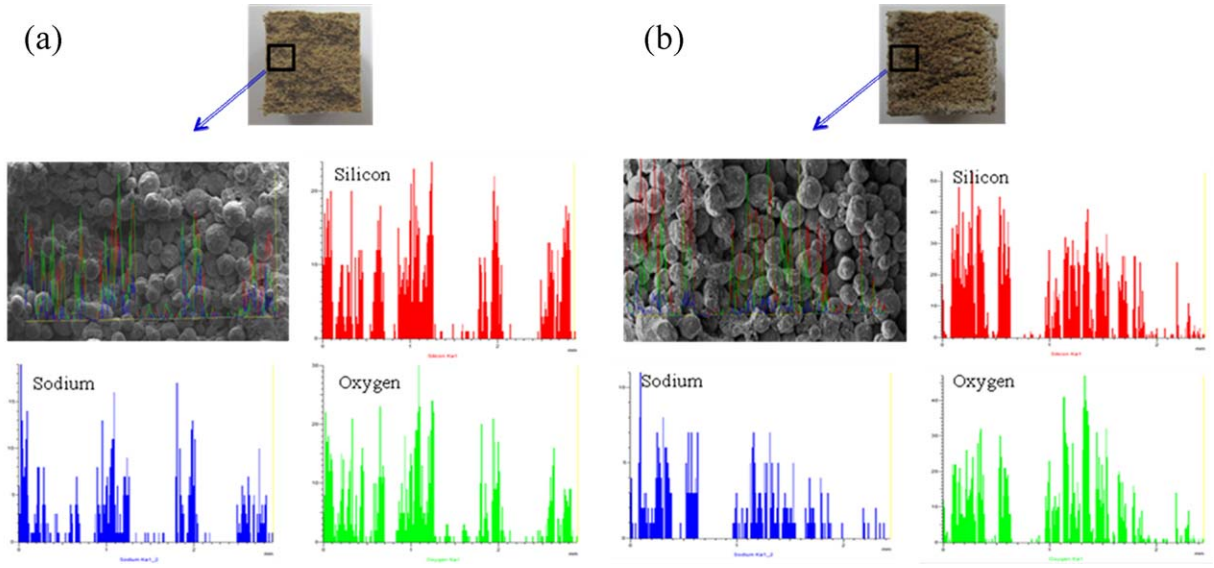

Fig. 6. Element analysis of each sample based on binder composition (Run 3): (a) before and (b) after heat treatment.

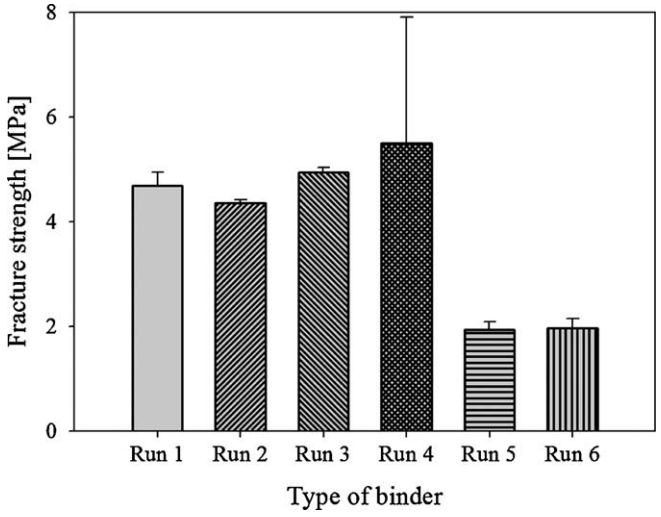

Fig. 7. Fracture strength of samples after heat treatment as a function of binder composition.

mobility, related to the reactivity of molecules. PVA and PDMS used as the organic and inorganic binders, respectively, have extremely high viscosities compared with TEOS. Therefore, the sample with the lowest viscosity (Run 4) obtained by process II has a similar fracture strength, of about 5 MPa, to samples obtained by process I, while samples having a relatively high viscosity (Runs 5 and 6) show a low strength because of the decrease in reactivity of precursors. Even though Run 4 shows a higher strength value, which is similar to samples without the organic binder (PVA), the in situ method of process I has an advantage in collapsibility of the mold after precision casting. Consequently, the viscosity of precursor used as a binder as well as the binder composition is important factors in preparing a mold with reasonable properties.

4. Conclusions

A new in situ process has been developed to decrease the processing time and production costs and produce an environmentally friendly mold, compared with the conventional process. In the new process, the starting powder is fastened by inorganic binders generated through a sol–gel reaction during a drying process, in contrast to the conventional mold process using an organic binder. Samples prepared by this process clearly show a reaction area of Na_2SiO_3 and/or SiO_2 owing to the variation in chemical potential of precursors, leading to similar fracture strength values independent of the binder composition. However, in the case of molds formed by addition of the organic binder, the reaction area is uniformly and homogeneously spread over the entire sample, attributed to the decrease in mobility of precursor in matrix because of the high viscosity. Consequently, it is an essential requirement for fabrication of a mold having desirable properties to consider the viscosity of the binder mixtures as well as the binder composition. In this work, samples with fracture strengths of about 5 MPa have been achieved through the in situ process, indicating that this new process, especially process I, can be applied to fabrication of molds having high mechanical–thermal properties for precision casting.

Acknowledgments

This work was supported by the Power Generation & Electricity Delivery (R-2007-1-003-02/2009T100200025) and Human Resources Development (2007-P-EP-HM-E-02-0000) of the Korean Institute of Energy Technology Evaluation and Planning (KETEP) grants, and Leading Industry Development for Economic Region (70007779) funded by the Korean Ministry of Knowledge Economy.

References

1. Meng YA, Thomas BG. Modeling transient slag-layer phenomena in the shell/mold gap in continuous casting of steel. *Metal Mater Trans B* 2003;**34B**:707–25.
2. Şimşir M, Kumruoğlu LC, Őzer A. An investigation into stainless-steel/structure-alloy-steel bimetal produced by shell mould casting. *Mater Des* 2009;**30**:264–70.
3. Barsoum M. *Fundamentals of ceramics*. Seoul: McGraw-Hill; 1997.
4. Callister WD. *Materials science and engineering: an introduction*. New York: Wiley; 1997.
5. Sasaki N. *A revolutionary inorganic core and mold making process*. Foundry Management & Technology; 2009.
6. Terry Lay GF, Rockwell MC, Wiltshire JC, Ketata C. Characteristics of silicate glasses derived from vitrification of manganese crust tailings. *Ceram Inter* 2009;**35**:1961.
7. Sahoo PK, Samal R, Swain SK, Rana PK. Synthesis of poly(butyl acrylate)/sodium silicate nanocomposite fire retardant. *Eur Polym J* 2008;**44**:3522.
8. Sandhu AK, Singh W, Pandey OP. Neutron irradiation effects on optical and structural properties of silicate glasses. *Mater Chem Phys* 2009;**115**:783.
9. Shi X, Xu S, Lin J, Feng S, Wang J. Synthesis of SiO_2–polyacrylic acid hybrid hydrogel with high mechanical properties and salt tolerance using sodium silicate precursor through sol–gel process. *Mater Lett* 2009;**63**:527.
10. Chen Y, Hong Y, Zheng F, Li J, Wu Y, Li L. Preparation of silicate stalagmite from sodium silicate. *J Alloys Compd* 2009;**478**:411.
11. Gurav JL, Rao AV, Rao AP, Nadargi DY, Bhagat SD. Physical properties of sodium silicate based silica aerogels prepared by single step sol–gel process dried at ambient pressure. *J Alloys Compd* 2009;**476**:397.
12. Anbia M, Lashgari M. Synthesis of amino-modified ordered mesoporous silica as a new nano sorbent for the removal of chlorophenols from aqueous media. *Chem Eng J* 2009;**150**:555.
13. Xue W, Bandyopahyay A, Bose S. Mesoporous calcium silicate for controlled release of bovine serum albumin protein. *Acta Biomater* 2009;**5**:1686.
14. Silbey RJ, Alberty RA. *Physical chemistry*. New York: John Wiley & Sons, Inc.; 2001.
15. Goodwin JW, Hughes RW. *Rheology for chemists: an introduction*. Cambridge: The Royal Society of Chemistry; 2000. p. 9.
16. Sumana G, Raina KK. Electro-optic properties of aligned polysiloxane dispersed ferroelectric liquid crystal composite thin films. *Curr Appl Phys* 2005;**5**:277.